Full QED + QCD Low-Energy Constants through Reweighting

Tomomi Ishikawa,[1,2] Thomas Blum,[2] Masashi Hayakawa,[3,4] Taku Izubuchi,[1,5] Chulwoo Jung,[5] and Ran Zhou[6]
[1]*RIKEN BNL Research Center, Brookhaven National Laboratory, Upton, New York 11973, USA*
[2]*Physics Department, University of Connecticut, Storrs, Connecticut 06269-3046, USA*
[3]*Department of Physics, Nagoya University, Nagoya 464-8602, Japan*
[4]*Nishina Center, RIKEN, Wako, Saitama 351-0198, Japan*
[5]*Physics Department, Brookhaven National Laboratory, Upton, New York 11973, USA*
[6]*Physics Department, Indiana University, Bloomington, Indiana 47405, USA*
(Received 2 March 2012; published 16 August 2012)

The effect of sea quark electromagnetic charge on meson masses is investigated, and first results for full QED + QCD low-energy constants are presented. The electromagnetic charge for sea quarks is incorporated in quenched QED + full QCD lattice simulations by a reweighting method. The reweighting factor, which connects quenched and unquenched QED, is estimated using a stochastic method on 2 + 1 flavor dynamical domain-wall quark ensembles.

DOI: 10.1103/PhysRevLett.109.072002 PACS numbers: 12.38.Gc, 12.39.Fe

So far, most lattice QCD simulations have been performed neglecting the electromagnetic (EM) charges. In order to calculate physical quantities to high precision, it is quite important to include and control this contribution. Toward this goal, several attempts regarding this issue have been done using quenched QED [1–5].

Chiral perturbation theory (ChPT) provides an effective guide to extrapolate to the physical quark mass point in a lattice calculation, and in combination with QED, is a powerful tool for addressing isospin breaking. The QED effect can be included in the ChPT framework: partially quenched ChPT (PQChPT) with QED was first derived by Bijnens and Danielsson [6] in the $SU(3)$ flavor basis up to next-to-leading order (NLO) and was recently extended by some of us to the $SU(2)$ flavor + kaon basis [4]. In PQChPT, sea and valence quarks are separately treated. Here, we specify the two valence quarks in mesons by indices 1 and 3 and the three sea quarks (u, d, s) by indices 4–6, and then introduce quark masses m_i and quark EM charges q_i in units of the fundamental EM charge e. Distinguishing formally the fundamental charges in the sea quark sectors, e_s, and in the valence quark sectors, e_v, NLO $SU(3)$ PQChPT tells us the sea EM charge contribution to the pseudo-scalar (PS) meson mass-squared is

$$\begin{aligned}\Delta(M_{\rm PS}^{SU(3)})^2 &= (M_{\rm PS}^{SU(3)}[e_s \neq 0, e_v \neq 0])^2 \\ &\quad - (M_{\rm PS}^{SU(3)}[e_s = 0, e_v \neq 0])^2 \\ &= -4e_s^2 Y_1 {\rm tr} Q_{s(3)}^2 \chi_{13} \\ &\quad + e_s e_v \frac{C}{F_0^4}\frac{1}{8\pi^2}\sum_{i=4,5,6}\left(\chi_{1i}\ln\frac{\chi_{1i}}{\mu^2} - \chi_{3i}\ln\frac{\chi_{3i}}{\mu^2}\right) \\ &\quad \times q_i(q_1 - q_3), \end{aligned} \quad (1)$$

with $\chi_{ij} = B_0(m_i + m_j)$, $Q_{s(3)} = {\rm diag}(q_4, q_5, q_6)$. μ is an energy scale below which the effective theory accurately describes the theory (QED + QCD), and B_0, F_0, C and Y_1 are low-energy constants (LECs). Determination of Y_1 requires $e_s \neq 0$, which is not accessible in quenched QED (qQED). Note that the LECs generally depend on masses and EM charges of heavier dynamical quarks than u, d, and s. In the following, three-flavors of dynamical quarks are assumed: u, d, and s. We also mention that a remarkable feature in the three-flavor theory,

$$ {\rm tr}\, Q_{s(3)} = 0, \quad (2)$$

makes many terms vanish and leads to the simple form in Eq. (1). Recently, RBC and UKQCD collaborations pointed out that the $SU(2)$ ChPT is preferable to the $SU(3)$ ChPT even in the three-flavor full QCD (fQCD) simulation, since the s quark mass is not small enough [7]. In this case, the sea EM contribution to a pion mass-squared, for example, can be written as

$$\begin{aligned}&\Delta(M_\pi^{SU(2)})^2 \\ &= -4e_s^2\{Y_1 {\rm tr} Q_{s(2)}^2 + Y_1'({\rm tr} Q_{s(2)})^2 + Y_1'' q_6 {\rm tr} Q_{s(2)}\}\chi_{13} \\ &\quad + e_s e_v\left\{\frac{C}{F_0^4}\frac{1}{8\pi^2}\sum_{i=4,5}\left(\chi_{1i}\ln\frac{\chi_{1i}}{\mu^2} - \chi_{3i}\ln\frac{\chi_{3i}}{\mu^2}\right)q_i \right. \\ &\quad \left. + 4(\chi_1 - \chi_3)(J{\rm tr}Q_{s(2)} + J' q_6)\right\}(q_1 - q_3) \\ &\quad + 4e_s e_v(K {\rm tr} Q_{s(2)} + K' q_6)(q_1 + q_3)\chi_{13}, \end{aligned} \quad (3)$$

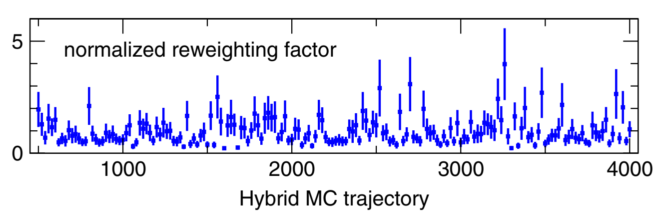

FIG. 1 (color online). Normalized reweighting factor $w[\tilde{U}, U]$ with the EM charge $e_s = e$ on each gluon configuration.

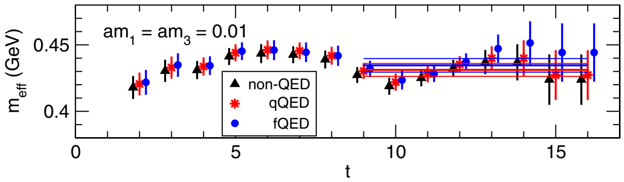

FIG. 2 (color online). An example of effective mass for the π^+ meson in non-QED (black), qQED (red), and fQED (blue) with $am_1 = am_3 = 0.01$. The χ^2 fit results of the masses with an uncorrelated fit in t are denoted by the horizontal lines. In fitting the fQED data, $\chi^2/\text{d.o.f.(uncorr)} = 0.11$ and $\chi^2/\text{d.o.f.(corr)} = 0.67$.

where $\chi_i = 2B_0 m_i$, $Q_{s(2)} = \text{diag}(q_4, q_5)$. We remark that additional LECs, Y_1', Y_1'', J, J', K and K' to Eq. (1) arise due to lack of the property (2) in the $SU(2)$ case, and the LECs in Eq. (3) generally depend on a mass and an EM charge of the s quark.

While the full QED (fQED) effect can be incorporated in the Monte Carlo evolution of the gauge field configuration, the usual gauge ensemble has been generated only with dynamical QCD. However, the fQED effect, in principle, can be included using a reweighting method [8]. The main purpose of this work is to show the practicality of the reweighting method for incorporating the sea quark EM charge on a domain-wall fermion (DWF) ensemble originally generated with $e_s = 0$ and the feasibility of obtaining the fQED LECs. (Some applications of reweighting to a realistic QED + QCD simulation were recently reported in Refs. [9,10].) Full theory includes a $U(1)$ photon field A in addition to the usual $SU(3)$ link variable U for the gluon field and fermion field ψ. In order to illustrate the reweighting method, we consider the system with a fermion action $S_f[\bar\psi, \psi, \tilde U] = -\bar\psi D[\tilde U]\psi$, where $\tilde U$ is the combined $SU(3) \times U(1)$ gauge link variable associated with a quark with EM charge qe;

$$\tilde U = U e^{iqeA}. \tag{4}$$

Here, we assume the photon fields are generated by a non-compact $U(1)$ photon action;

$$S_{U(1)}[A] = \frac{1}{4}\sum_x \sum_{\mu,\nu} (\partial_\mu A_\nu(x) - \partial_\nu A_\mu(x))^2. \tag{5}$$

In this study the fine structure constant of QED is set to be $\alpha_{\text{EM}} = e^2/(4\pi) = 1/137$. An expectation value for some observable O in fQED + fQCD is formally related to the one in qQED + fQCD, in which the photon fields in the quark determinants are neglected, via

$$\langle O\rangle_{\text{fQED+fQCD}} = \frac{\langle wO\rangle_{\text{qQED+fQCD}}}{\langle w\rangle_{\text{qQED+fQCD}}}, \tag{6}$$

introducing a reweighting factor [8],

$$w[\tilde U, U] = \frac{\det(D[\tilde U])}{\det(D[U])}. \tag{7}$$

The determinants in Eq. (7) are calculated by a stochastic estimate with random Gaussian noise vectors. Since the distribution of w has a long tail, a naive application of the stochastic estimator for w could fail [11]. To evaluate w safely, breaking up the determinant into many small pieces is efficient, because the effects of the outliers are largely suppressed [11,12]. For the splitting, we use a mathematical identity for the determinant, so called the nth-root trick: $w = \det\Omega = (\det\Omega^{1/n})^n$, which is easily implemented by the rational approximation [13]. We apply reweighting to 2 + 1 flavor dynamical DWF and Iwasaki gluon configurations generated by the RBC-UKQCD collaborations [14]. The configuration set is one of the ensembles used in the qQED study [4], whose simulation parameters are $\beta_{\text{QCD}} = 2.13$, $L^3 \times T \times L_s = 16^3 \times 32 \times 16$, inverse lattice spacing $a^{-1} = 1.784(44)$ GeV, $(am_u, am_d, am_s) = (0.01, 0.01, 0.04)$. The $U(1)$ photon fields, which have

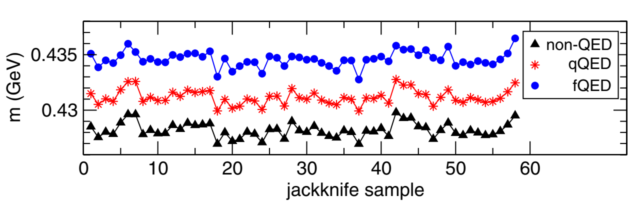

FIG. 3 (color online). Jackknife data of fit masses of Fig. 2 (uncorr).

TABLE I. Transformation property under Eqs. (12)–(14) for individual terms in NLO $SU(3)$ and $SU(2)$ PQChPT.

Transformation	Terms in NLO PQChPT associated with Y_1, Y_1', Y_1''	$C, \mathcal{J}, \mathcal{J}'$	$\mathcal{K}, \mathcal{K}'$
$\mathcal{T}_1$ [Eq. (12)]	even	even	even
$\mathcal{T}_2$ [Eq. (13)]	even	odd	odd
$\mathcal{T}_3$ [Eq. (14)]	even	even	odd

TABLE II. QED low-energy constants with $\mu = \Lambda_\chi = 1$ GeV. $\mathcal{Y}_1$ is defined as $\mathcal{Y}_1 = Y_1 \text{tr} Q_{s(3)}^2$ for $SU(3)$ ChPT and $\mathcal{Y}_1 = Y_1 \text{tr} Q_{s(2)}^2 + Y_1'(\text{tr}Q_{s(2)})^2 + Y_1'' q_6 \text{tr}Q_{s(2)}$ for $SU(2)$ ChPT. $\mathcal{J}$ and $\mathcal{K}$ depict $\mathcal{J} = J\text{tr}Q_{s(2)} + J'q_6$ and $\mathcal{K} = K\text{tr}Q_{s(2)} + K'q_6$, respectively. The qQED values for C are quoted from Ref. [4], whose values are obtained from the $24^3 \times 64$ lattice and by the infinite volume ChPT formula. The values of B_0 and F_0 used in the chiral fit are quoted from Ref. [7].

	$SU(3)$ ChPT uncorr	$SU(3)$ ChPT corr	$SU(2)$ ChPT uncorr	$SU(2)$ ChPT corr
$10^7 C$ (qQED)	2.2(2.0)	⋯	18.3(1.8)	⋯
$10^7 C$	8.4(4.3)	8.3(4.7)	20(14)	15(21)
$10^2 Y_1$	−5.0(3.6)	−0.4(5.6)	⋯	⋯
$10^2 \mathcal{Y}_1$	−3.1(2.2)	−0.2(3.4)	−3.0(2.2)	−0.2(3.4)
$10^4 \mathcal{J}$	⋯	⋯	−2.6(1.6)	−3.3(2.8)
$10^4 \mathcal{K}$	⋯	⋯	−3.1(6.9)	−3.7(7.8)

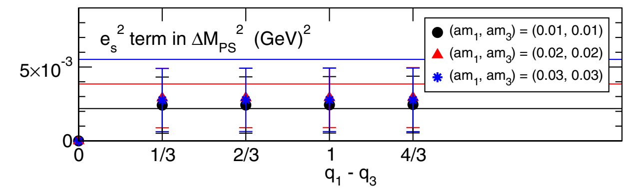

FIG. 4 (color online). e_s^2 contribution to $M_{\rm PS}^2$ (uncorr). The lines represent uncorrelated fits to $SU(2)$ PQChPT.

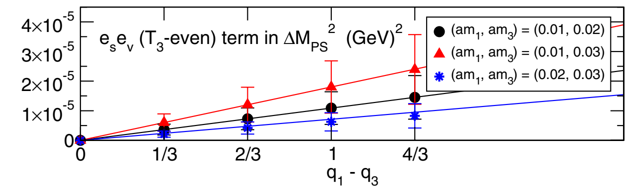

FIG. 6 (color online). $e_s e_v$ ($\mathcal{T}_3$-even) contribution to $M_{\rm PS}^2$ (uncorr). Lines represent uncorrelated fits to $SU(2)$ PQChPT.

been already generated in the qQED study, are combined with the gluon configurations according to Eq. (4). We also employ $n = 24$ roots and use 4 complex random Gaussian noise vectors per root on each configuration to estimate the reweighting factors. Figure 1 shows the obtained factors normalized by the configuration average. The fluctuation among configurations is moderate, controlled within a factor of ~5.

DWFs explicitly break chiral symmetry due to finite size L_s in the extra 5th dimension which can be quantified by an additive, residual, quark mass for each flavor. In the chiral limit, $am_{\rm res(QCD)} = 0.003\,148(46)$ for the ensemble used in this study. The qQED studies [3,4] show that the valence EM charges further shift the quark mass by an amount of $\mathcal{O}(\alpha_{\rm EM} am_{\rm res(QCD)})$. The same effect also arises from the sea quark charges. This lattice artifact induces a term like $e_s^2 \delta_{\rm res} {\rm tr} Q_{s(3)}^2$ in the $SU(3)$ ChPT formula (1). [Similar modifications are also needed in the $SU(2)$ formula (3).] Here we measure the sea EM charge contribution to the residual mass and subtract it from $\Delta M_{\rm PS}^2$.

Due to finiteness of gauge configurations, contributions arise from "hair," or photon emission to, and absorption from, the vacuum which averages to zero in the large ensemble limit. In Ref. [3], it was shown that this hair is a large source of noise in hadron correlators. The leading unwanted piece can, however, be removed by averaging over plus and minus EM charges, the so-called $\pm e$ trick, and it provides a great advantage in which the unphysical noise is exactly canceled in the valence sector [3,4];

$$\tfrac{1}{2}\{O(+e_v) + O(-e_v)\} = \mathcal{O}(e_v^2), \qquad (8)$$

where $O(e_v)$ represents some observable with a valence EM charge e_v. There is also "hair" in the sea sector. To remove the leading contribution from both the sea and valence sectors, we use an averaging,

$$\tfrac{1}{2}\{O(+e_s, +e_v) + O(-e_s, -e_v)\} = \mathcal{O}(e_s^2, e_s e_v, e_v^2), \qquad (9)$$

in the reweighting. Note that the noise from hair associated with e_s is already small by virtue of Eq. (2).

Using the reweighting factor obtained in this work and the meson correlators in the qQED study [4], the reweighted meson correlators are obtained by Eq. (6). An example of effective mass for the π^+ meson is shown in Fig. 2. For the χ^2 fit results of the masses, we take the same fit range ($t = 9$–16) as in Ref. [4] and also perform both correlated (corr) and uncorrelated (uncorr) fits in t. (Changing the fit range does not alter results beyond the current statistical error.) To study the properties of the data, we show jackknife samples of fit masses from Fig. 2 in Fig. 3. Figure 3 indicates that the statistical fluctuation comes mostly from QCD and that significant correlations exist between the charged and non-charged data. These facts enable us to detect the qQED and fQED effects. With the reweighted data of the meson masses calculated, chiral fits are performed to obtain the QED LECs in Eqs. (1) and (3). Although C is known from the qQED study [4], it provides a valuable consistency check with the qQED result. In fitting for the LECs, we anticipated a problematic hierarchy between the e_s^2 and $e_s e_v$ terms, attributable to a double suppression factor in the latter,

$$\frac{m_1 - m_3}{m_1 + m_3} {\rm tr}(Q_{s(3)} M_{s(3)}) \frac{\bar{m}}{\Lambda_{\rm QCD}}, \qquad (10)$$

leaving the $e_s e_v$ terms unresolved, where

$$M_{s(3)} = \frac{1}{\bar{m}} {\rm diag}(m_4, m_5, m_6), \quad \bar{m} = \frac{m_4 + m_5 + m_6}{3}. \qquad (11)$$

Although the difficulty can, in principle, be overcome with enormous statistics, drastic improvements are provided by engineering sign flips in the EM charge. Besides the $\pm e$ trick [Eqs. (8) and (9)], consider a basic transformation

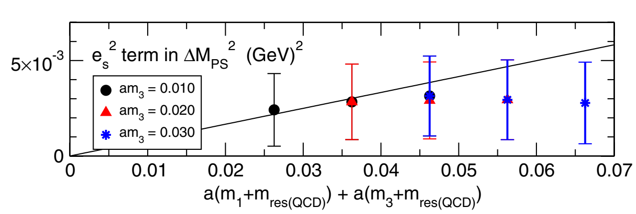

FIG. 5 (color online). Same as Fig. 4 but for $(q_1, q_3) = (+2/3, -1/3)$, showing the valence quark mass dependence.

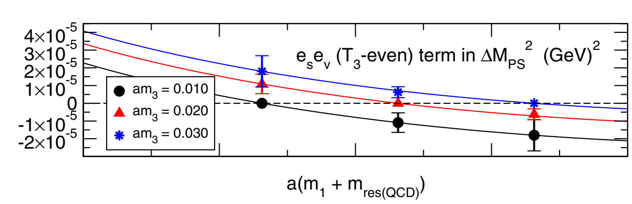

FIG. 7 (color online). Same as Fig. 6 but for $(q_1, q_3) = (+2/3, -1/3)$, showing the valence quark mass dependence.

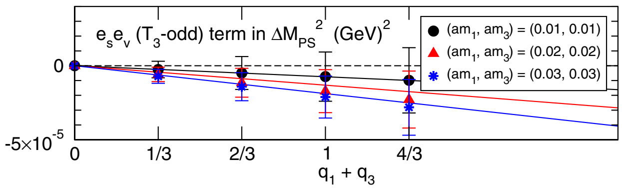

FIG. 8 (color online). $e_s e_v$ ($\mathcal{T}_3$-odd) contribution to $M_{\rm PS}^2$ (uncorr). The lines represent uncorrelated fits to $SU(2)$ PQChPT.

$$\mathcal{T}_1:(m_1, q_1; m_3, q_3) \to (m_3, q_3; m_1, q_1), \tag{12}$$

under which the meson system is invariant (CPT). In addition to $\mathcal{T}_1$, let us introduce transformations:

$$\mathcal{T}_2:(m_1, q_1; m_3, q_3) \to (m_1, -q_1; m_3, -q_3), \tag{13}$$

$$\mathcal{T}_3:(m_1, q_1; m_3, q_3) \to (m_3, -q_1; m_1, -q_3). \tag{14}$$

Equations (12)–(14) form a set of transformations that exchange two valence quark masses and EM charges with, or without, flipping the sign of e_v. Note that $\mathcal{T}_2$ and $\mathcal{T}_3$ yield only partial invariances of Eqs. (1) and (3), in the sense that the invariance holds only for specific terms in each. In Tab. I, the transformation property of each term in NLO PQChPT is summarized. While the e_s^2 and $e_s e_v$ terms retain their even and oddness under $\mathcal{T}_1$ and $\mathcal{T}_2$ to all orders in quark mass, the transformation property under $\mathcal{T}_3$ is not preserved at order higher than $O(am)$ in the quark mass expansion. At NLO in $SU(2)$ PQChPT in formula (3), the $e_s e_v$ term is a mixture of even and odd contributions since the three-flavor feature (2) is explicitly broken. By adding and subtracting squared meson masses related by these transformations, each term can be separately extracted and individually fit. Note that we need at least three different sets of sea quark EM charges to fully determine the fQED LECs using the $SU(2)$ ChPT; otherwise we only know their linear combinations (see Tab. II). A useful choice would be: [tr$Q_{s(2)} = 0$, $\forall q_6$], [tr$Q_{s(2)} \neq 0$, $q_6 = 0$] and [tr$Q_{s(2)} \neq 0$, $q_6 \neq 0$].

Figures 4–9 show individual sea-quark charge contributions to the pion mass-squared, e_s^2, $e_s e_v$ ($\mathcal{T}_3$-even) and $e_s e_v$ ($\mathcal{T}_3$-odd) parts. The lattice artifact ingredient, which is caused by the finiteness of L_s, is subtracted from the e_s^2 term. In the figures, we can clearly see that the hierarchy between the e_s^2 and $e_s e_v$ terms is $\mathcal{O}(10^2)$, as expected by the suppression given by Eq. (10), and the separation using the transformation $\mathcal{T}_2$ successfully works. The valence

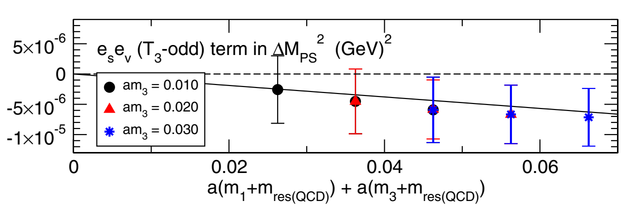

FIG. 9 (color online). Same as Fig. 8 but for $(q_1, q_3) = (+2/3, +1/3)$, showing the valence quark mass dependence.

EM charge dependence is constant for the e_s^2 term and linear for the $e_v e_s$ terms, as expected from the smallness of the fine structure constant in QED. We perform uncorrelated chiral fits for the e_s^2, $e_s e_v$ ($\mathcal{T}_3$-even) and $e_s e_v$ ($\mathcal{T}_3$-odd) terms separately setting μ to the chiral scale $\Lambda_\chi = 1$ GeV and obtain the LECs in Tab. II. In this fit, we choose a minimal set of data with smaller valence quark masses, and ignore q_6 dependence in B_0 because of smallness of e^2 and Y_1. We also neglect finite volume effects which could give significant shifts in the EM mass spectrum. However, we remark that our quarks are relatively heavy even though our lattice is small. Although the statistical error is large, the value of LEC C is consistent with that obtained in qQED [4]. (The lattice volume and the quark masses used in the chiral fit are different between this work and Ref. [4]. The important fact, however, is that the order of magnitude is consistent between them.) The size of Y_1 seems to be the same as the other QED LECs in $\mathcal{O}(e_v^2 m)$ terms determined in qQED [4], which means the sea EM charge effect is comparable to the valence one except for the Dashen term.

In this study, incorporating sea quark EM charges in 2 + 1 flavor lattice QED + QCD, we have shown that the QED LECs are accessible using the reweighting method, and that the sea quark LECs are the same size as the valence ones, as expected. In our analysis, the sign flip engineering of EM charges proved to be highly effective, similar to the $\pm e$ trick for the valence sector [3,4]. Since this is a first computation of sea EM charge effects in large scale computation, our primary aim is to show the method works and the size of the statistical error. Checks for systematic errors including the discretization error, which is a few percent on this lattice for pure QCD [15], finite volume, and so on, are being investigated on larger lattices, $24^3 \times 64$ and $32^3 \times 64$. Implementation of further algorithmic improvements, for example, low-mode averaging to increase statistics, are also in progress.

We are grateful to USQCD and the RBRC for providing computer time on the DOE and RBRC QCDOC supercomputers at BNL for the computations reported here. T. B. and T. Ishikawa were supported by the U.S. DOE under Grant No. DE-FG02-92ER40716. M. H. is supported by JSPS Grants-in-Aid for Scientific Research No. (S) 22224003 and No. (C)20540261. T. Izubuchi is partially supported by JSPS Kakenhi Grants No. 22540301 and No. 23105715. T. Izubuchi and C. J. are supported by the DOE under Contract No. DE-AC02-98CH10886.

[1] A. Duncan, E. Eichten, and H. Thacker, Phys. Rev. Lett. **76**, 3894 (1996).
[2] A. Duncan, E. Eichten, and H. Thacker, Phys. Lett. B **409**, 387 (1997).
[3] T. Blum, T. Doi, M. Hayakawa, T. Izubuchi, and N. Yamada, Phys. Rev. D **76**, 114508 (2007).

[4] T. Blum, R. Zhou, T. Doi, M. Hayakawa, T. Izubuchi, S. Uno, and N. Yamada, Phys. Rev. D **82**, 094508 (2010).
[5] A. Torok *et al.*, Proc. Sci., LATTICE 2010 (2010) 127.
[6] J. Bijnens and N. Danielsson, Phys. Rev. D **75**, 014505 (2007).
[7] C. Allton *et al.* (RBC-UKQCD Collaboration), Phys. Rev. D **78**, 114509 (2008).
[8] A. Duncan, E. Eichten, and R. Sedgewick, Phys. Rev. D **71**, 094509 (2005).
[9] A. Portelli *et al.* (Budapest-Marseille-Wuppertal Collaboration), Proc. Sci., LATTICE 2010 (2010) 121.
[10] N. Ukita (The PACS-CS Collaboration), Proc. Sci., Lattice 2011 (2011) 144.
[11] T. Ishikawa *et al.*, Proc. Sci., LAT2009 (2009) 035.
[12] A. Hasenfratz, R. Hoffmann, and S. Schaefer, Phys. Rev. D **78**, 014515 (2008).
[13] M. A. Clark and A. D. Kennedy, Phys. Rev. Lett. **98**, 051601 (2007).
[14] C. Allton *et al.* (RBC and UKQCD Collaborations), Phys. Rev. D **76**, 014504 (2007).
[15] Y. Aoki *et al.* (RBC and UKQCD Collaborations), Phys. Rev. D **83**, 074508 (2011).